

# Energy-efficient pathway for selectively exciting solute molecules to high vibrational states via solvent vibration-polariton pumping

Tao E. Li,<sup>1,\*</sup> Abraham Nitzan,<sup>1,2,†</sup> and Joseph E. Subotnik<sup>1,‡</sup>

<sup>1</sup>*Department of Chemistry, University of Pennsylvania, Philadelphia, Pennsylvania 19104, USA*

<sup>2</sup>*School of Chemistry, Tel Aviv University, Tel Aviv 69978, Israel*

Selectively exciting target molecules to high vibrational states is inefficient in the liquid phase, which restricts the use of IR pumping to catalyze ground-state chemical reactions. Here, we demonstrate that this inefficiency can be largely solved by confining the liquid in an optical cavity under vibrational strong coupling conditions. For a liquid solution of  $^{13}\text{CO}_2$  solute in a  $^{12}\text{CO}_2$  solvent, cavity molecular dynamics simulations show that exciting a polariton (hybrid light-matter state) of the solvent with an intense laser pulse, under suitable resonant conditions, may lead to a very strong ( $> 3$  quanta) and ultrafast ( $< 1$  ps) excitation of the solute, all while the solvent is barely excited. By contrast, outside a cavity the same input pulse fluence can excite the solute by only half a vibrational quantum and the selectivity of excitation is low. Our finding is robust under different cavity volumes, which may lead to observable cavity enhancement on IR photochemical reactions in Fabry-Pérot cavities.

## I. INTRODUCTION

Controlling (electronic) ground-state chemical reaction rates with an external infrared (IR) laser is a long-standing goal of IR photochemistry. Although it is possible to trigger chemical reactions by exciting the reactants to high vibrational excited states via ladder climbing [1], such IR-controlled chemical reactions are rarely efficient in the liquid phase because of competing relaxation processes that transfer vibrational energy to other degrees of freedom, either internal modes of the molecule or external modes of surrounding molecules (leading to build up of heat in the environment) [2]. Moreover, due to molecular anharmonicity, exciting reactants to high vibrational excited states requires a wide-band IR pulse, but such a wide-band pulse can also often directly excite solvent molecules as well. Up to now, there have been only a few observations of selective IR photochemistry (i.e. reactions where an IR pump promotes selective reactions beyond a simple heating effect) [3, 4]. Recent experiments by Weinstein *et al* [5] have concluded that, with proper IR pumping, one can achieve modest increases in electron transfer rates after applying a subsequent UV pulse. That being said, if there were a general mechanism for targeting some molecules (e.g., reactants or solute molecules) and achieving highly vibrationally excited states on a timescale shorter than the lifetime of vibrational energy relaxation, one could imagine using IR (or perhaps IR followed by UV) light to help catalyze reactions of interest.

In this manuscript, we address this question of vibrationally targeting solute molecules by exciting a solvent vibrational polariton [6, 7] inside an optical cavity. Forming vibrational polaritons — the hybrid light-matter states — requires strong light-matter interactions,

which can be realized by confining a large ensemble of molecules inside an optical cavity and when a vibrational mode of molecules is near resonant with a cavity mode. In this collective vibrational strong coupling (VSC) regime, recent experimental results [8–11] indicate that forming polaritons can have a substantial effect on thermally-activated ground-state chemical reactions even in relative large Fabry-Pérot microcavities (i.e., a pair of macroscopic parallel mirrors with a spacing of micrometers) and without external laser pumping, although theoretical considerations have so far failed to explain these observations [12–16]. Recent work by Xiang *et al* has investigated the possibility of accelerating intermolecular vibrational energy transfer [17] by pumping the upper vibrational polariton (UP) with an external IR laser. Thus, within the context of polariton chemistry, one must also wonder whether VSC can be used as a tool to modify reactivity pathways for solute molecules and promote thermal chemistry under IR excitation.

Here, we will numerically show that collective VSC can provide such a mechanism to highly excite the vibration of target molecules — a small concentration of solute molecules — and leave the vast majority of solvent molecules barely excited. In order to demonstrate this energy-economic approach under VSC, we will focus on a molecular system with a small concentration of  $^{13}\text{CO}_2$  molecules dissolved in liquid  $^{12}\text{CO}_2$ . For this system, we will demonstrate that, in a suitable cavity environment, by exciting the solvent lower polariton (LP) with an intense IR laser pulse, each  $^{13}\text{CO}_2$  solute molecule can be transiently excited by more than three vibrational quanta, an energy which is more than fifty times larger than the  $^{12}\text{CO}_2$  solvent molecules, and this vast energy difference occurs mostly within 1 ps, a timescale usually shorter than the lifetime of vibrational energy relaxation. Moreover, the relative excitation of the solute increases when the solvent concentration increases. Outside the cavity, similar selectivity cannot be achieved and excitation of the solute molecules to high vibrational states requires more energy. In short, exciting the polariton provides a novel and efficient approach to selectively in-

\* taoli@sas.upenn.edu

† anitzan@sas.upenn.edu

‡ subotnik@sas.upenn.edu

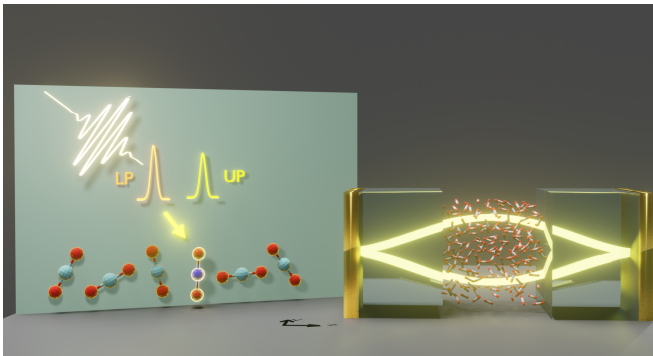


FIG. 1. Sketch of the cavity setup for CavMD simulations.  $N_{\text{cell}}$  molecules are confined in a cavity formed by a pair of parallel metallic mirrors. These molecules are coupled to a single cavity mode (with two polariton directions) and are simulated in a periodic simulation cell. The right cartoon demonstrates the main finding of this manuscript — after a strong excitation of the solvent lower polariton (LP) with an IR laser pulse, the input energy can be selectively transferred to the solute molecules solely, leaving the vast majority of solvent molecules barely excited.

put energy to solute molecules, and this finding is *independent* of the molecular system size and cavity volume (assuming constant density). Therefore, we believe this finding can be experimentally verified in both Fabry-Pérot and plasmonic cavities and with the potential of a large-scale application.

## II. METHODS

Our numerical approach is classical cavity molecular dynamics (CavMD) simulation [16, 18], our newly proposed tool for propagating the coupled photon-nuclear dynamics for realistic molecules within the limitations of a classical force field. This approach is formulated in the dipole gauge and includes the self-dipole term in the light-matter Hamiltonian, thus preserving gauge invariance. So far, CavMD has correctly captured some key features of both equilibrium and nonequilibrium VSC experiments [9, 19, 20], including (i) the asymmetry of a Rabi splitting [16], (ii) polaritonic relaxation to vibrational dark modes on a timescale of ps or sub-ps [18], and (iii) polariton-enhanced molecular nonlinear absorption [18] — a phenomenon whose signature is a delayed population gain in the first excited state of vibrational dark modes after strongly exciting the LP [20].

The fundamental equations underlying CavMD and all simulation details for exciting a polariton in a liquid carbon dioxide system (including the force field) can be found in Refs. [16, 18]. In short, as shown in Fig. 1, we imagine  $N_{\text{sub}}$  molecules in a periodic simulation cell coupled to a single cavity mode (with two polarization directions). The effective coupling strength between each molecule and the cavity mode is denoted as  $\tilde{\varepsilon}$ , which is

defined as

$$\tilde{\varepsilon} \equiv \sqrt{N_{\text{cell}}} \varepsilon. \quad (1)$$

Here,  $\varepsilon$  denotes the true light-matter coupling strength between each molecule and the cavity mode, and  $N_{\text{cell}}$  denotes the number of periodic simulation cells, the value of which can be determined by fitting the experimentally observed Rabi splitting. For the simulations below, by using an explicit force field, we include vibrational relaxation and dephasing for the molecular subsystem. We disregard cavity loss, which should usually be reasonable for Fabry-Pérot microcavities. Note that the main finding of this manuscript — selective polaritonic energy transfer to solute molecules — occurs mostly within 1 ps after the laser pumping, while a typical cavity mode lifetime for a Fabry-Pérot microcavity is  $\sim 5$  ps [20]. The code for reproducing this work, which is implemented based on the I-PI interference [21] and LAMMPS [22], is open-source available at Github [23].

## III. RESULTS AND DISCUSSION

### A. Polaritonic energy transfer in pure liquid

Before presenting the main finding of this manuscript — selective energy transfer to solute molecules — we investigate how exciting a polariton leads to a nonuniform energy redistribution in a pure liquid  $^{12}\text{CO}_2$  system (with  $N_{\text{sub}} = 216$  molecules explicitly propagated in a simulation cell) at room temperature (300 K). In Fig. 2a, we plot the equilibrium IR spectrum outside a cavity (black line) or inside a cavity (red line), where the IR spectrum is calculated by evaluating the auto-correlation function of the total dipole moment for the molecular subsystem [18, 24]. Inside the cavity, the C=O asymmetric stretch mode (peaked at  $\omega_0 = 2327 \text{ cm}^{-1}$ ) is resonantly coupled to a cavity mode (at  $\omega_c = 2320 \text{ cm}^{-1}$  corresponding to the vertical blue line) with an effective coupling strength  $\tilde{\varepsilon} = 2 \times 10^{-4}$  a.u.. In this collective VSC regime, a pair of LP ( $\omega_{\text{LP}} = 2241 \text{ cm}^{-1}$ ) and UP ( $\omega_{\text{UP}} = 2428 \text{ cm}^{-1}$ ) forms and these two peaks are separated by a Rabi splitting of  $187 \text{ cm}^{-1}$ .

We now excite the LP with a strong pulse of the form  $\mathbf{E}(t) = E_0 \cos(\omega t) \mathbf{e}_x$  ( $0.1 < t < 0.6$  ps) with fluence  $632 \text{ mJ/cm}^2$  ( $E_0 = 6 \times 10^{-3}$  a.u.). [This fluence will be used below and throughout the present manuscript except the choice of the frequency  $\omega$  (here  $\omega = \omega_{\text{LP}} = 2241 \text{ cm}^{-1}$ ), and the pulse is assumed to interact only with the molecular subsystem (there is no direct pulse-cavity interaction)]. In Fig. 2b, the resulting energy distribution is characterized by calculating the response of every  $^{12}\text{CO}_2$  molecule in the simulation cell after the LP excitation. The individual molecular response is calculated by evaluating the auto-correlation function of single-molecule dipole moment (which we call the "local" IR spectrum) [18] during a time window  $1 < t < 6$  ps (immediately after the LP excitation). In contrast to

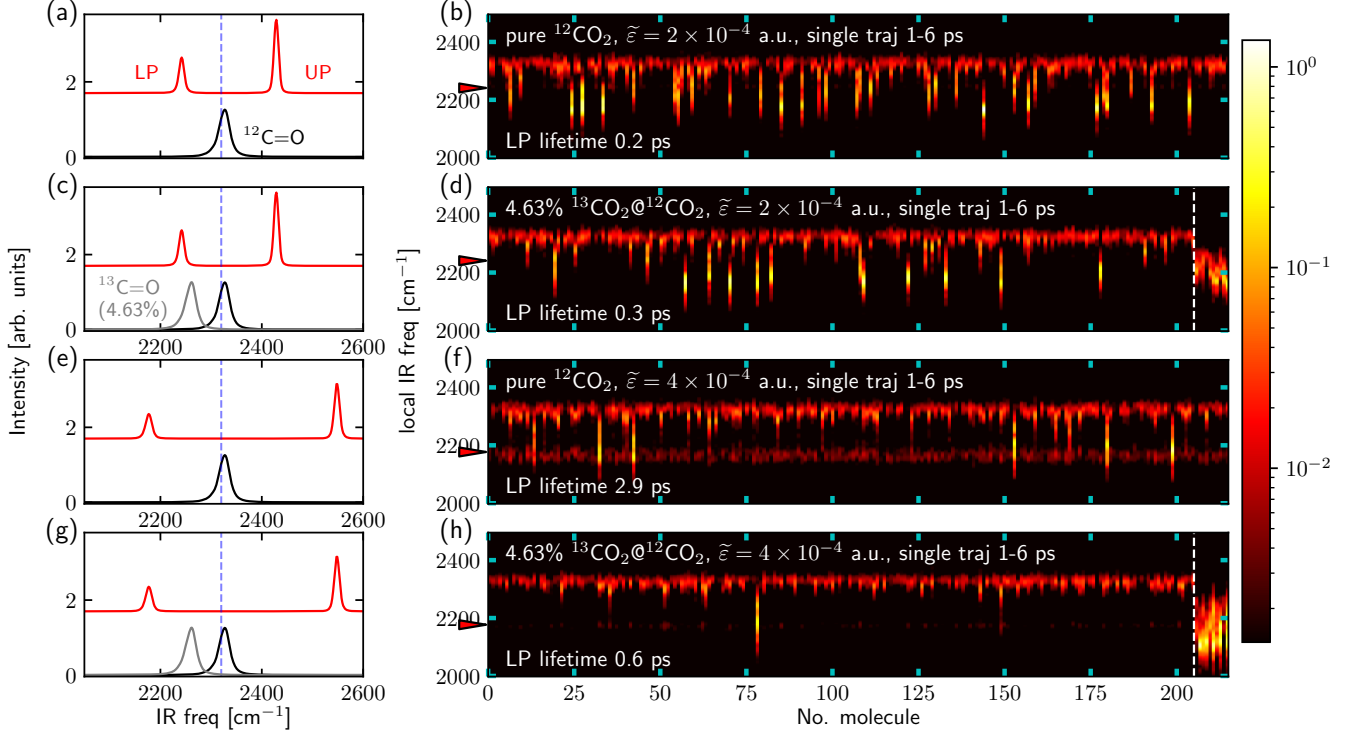


FIG. 2. Rabi splitting and selective polariton energy transfer. (a) Equilibrium IR spectrum for pure liquid <sup>12</sup>CO<sub>2</sub> outside a cavity (black line) or inside a cavity with  $\tilde{\epsilon} = 2 \times 10^{-4}$  a.u. (red line); the vertical dashed blue line denotes the cavity mode at 2320 cm<sup>-1</sup>. (b) The corresponding nonequilibrium local IR spectrum for each molecule after a resonant excitation of the LP at 2241 cm<sup>-1</sup> with a strong external pulse. The form of the external pulse takes  $E_0 \cos(\omega t + \phi) \mathbf{e}_x$  ( $0.1 < t < 0.6$  ps) with fluence 632 mJ/cm<sup>2</sup>. The nonequilibrium spectrum is calculated by evaluating the dipole auto-correlation function of each CO<sub>2</sub> molecule at time interval 1-6 ps. The red arrow marks the frequency of the LP and also the external pulse, and the LP lifetime (0.2 ps, calculated from photonic energy dynamics [18]) is labeled at the bottom. (c) Equilibrium IR spectrum (red line) for 4.63% <sup>13</sup>CO<sub>2</sub> in a <sup>12</sup>CO<sub>2</sub> solution when  $\tilde{\epsilon} = 2 \times 10^{-4}$  a.u.. The gray line denotes the <sup>13</sup>CO<sub>2</sub> IR spectrum outside the cavity; again, the black line denotes the pure <sup>12</sup>CO<sub>2</sub> IR spectrum outside the cavity. (d) The corresponding nonequilibrium local IR spectrum for each molecule plotted in a similar manner as Fig. b. The responses of <sup>12</sup>CO<sub>2</sub> (left) and <sup>13</sup>CO<sub>2</sub> (right) are separated by the vertical dashed white line. (e)-(h) The same plots as Figs. a-d accordingly but with a larger effective light-matter coupling ( $\tilde{\epsilon} = 4 \times 10^{-4}$  a.u.). Note that with an appropriate LP frequency, the LP is more likely to transfer energy to the <sup>13</sup>CO<sub>2</sub> solute molecules than the <sup>12</sup>CO<sub>2</sub> solvent. All simulation details are the same as Ref. [18].

the usual IR spectrum which is calculated by evaluating the auto-correlation function of the total dipole moment of a molecular system (as in Fig. 2a) and reflects the dynamics of the molecular bright mode, the local IR spectrum reflects the dynamics of individual molecules and can be expressed as a linear combination of molecular bright and dark modes. Because the total number of molecules explicitly accounted for in the simulation is large (with  $N_{\text{sub}} = 216$ ), the local IR spectrum is dominated by the density of dark modes.

In Fig. 2b, every column of pixels represents the local IR spectrum of one molecule (in total  $N_{\text{sub}} = 216$  molecules) during 1-6 ps and the colorbar (from red to orange) denotes a logarithmic scaled spectroscopic intensity. Clearly, after the LP excitation (where the LP lifetime fitted from photonic energy dynamics [18] is 0.2 ps), the polaritonic energy is nonuniformly transferred to different <sup>12</sup>CO<sub>2</sub> molecules (which are composed mostly of vibrational dark modes). While most molecules are only weakly excited and have a peak near 2320 cm<sup>-1</sup> (the equi-

librium IR peak; see also Fig. 2a), a dozen of molecules are strongly excited and show an intense, red-shifted peak near 2200 cm<sup>-1</sup>. Because we use an anharmonic force field [18] to simulate carbon dioxide molecules, the presence of intense, red-shifted peaks implies that the LP energy is mostly transferred to a small fraction of <sup>12</sup>CO<sub>2</sub> molecules.

The nonuniform polaritonic energy redistribution in Fig. 2b stems from polariton-enhanced molecular nonlinear absorption, a mechanism which has been shown experimentally (via two-dimensional IR spectroscopy) [20], analytically [25], and numerically (via CavMD) [18]. Quantum-mechanically speaking, when twice the LP energy roughly matches the  $0 \rightarrow 2$  vibrational transition of molecules, the LP can serve as a "virtual state" to enhance molecular nonlinear absorption of light and directly create highly vibrational excited molecules within a sub-ps timescale. In the present case (see Fig. 2a), the LP frequency sits between the fundamental <sup>12</sup>C=O

asymmetric stretch ( $\omega_0 = 2327 \text{ cm}^{-1}$ ) and  $1 \rightarrow 2$  vibrational transition (which is roughly  $2200 \text{ cm}^{-1}$ ). Hence, polariton-enhanced molecular nonlinear absorption can occur once the LP is strongly excited. Moreover, since molecules have different orientations and different local electrostatic environments (which leads to different instantaneous vibrational frequencies), only a small subset of molecules can interact strongly with the LP through the nonlinear channel (which requires an exact frequency match), thus leading to the vast difference in energy redistribution among molecules. In the end, some solvent molecules become highly excited and others do not.

## B. Polaritonic energy transfer to solute molecules

Let us now show that the mechanism above can be utilized to selectively transfer the energy from an IR laser pulse to a few target molecules in a liquid system. For the sake of simplicity, let us choose these target molecules to be a few  $^{13}\text{CO}_2$  molecules and investigate how to achieve selective energy transfer to these  $^{13}\text{CO}_2$  solute molecules (which are dissolved in a liquid  $^{12}\text{CO}_2$  solution).

For a solution of 4.63 % (10/216)  $^{13}\text{CO}_2$  molecules dissolved in liquid  $^{12}\text{CO}_2$  (in total  $N_{\text{sub}} = 216$  molecules are included in the simulation cell), the red line in Fig. 2c plots the equilibrium IR spectrum inside the same cavity as in Figs. 2a,b (with  $\omega_c = 2320 \text{ cm}^{-1}$  and  $\tilde{\epsilon} = 2 \times 10^{-4}$  a.u.). Because the concentration of the  $^{13}\text{CO}_2$  solute is small, inside the cavity, the positions of the polaritons are largely unchanged compared with the case of pure liquid  $^{12}\text{CO}_2$  (in Fig. 2a). Note that the equilibrium IR spectrum for pure liquid  $^{13}\text{CO}_2$  system outside a cavity is also plotted as the gray line in Fig. 2c, where the  $^{13}\text{C}=\text{O}$  asymmetric stretch peaks at  $2262 \text{ cm}^{-1}$ .

For this liquid mixture, after a strong excitation of the LP (again with a pulse fluence of  $632 \text{ mJ/cm}^2$ ), Fig. 2d plots the transient local IR spectra for every  $^{12}\text{CO}_2$  and  $^{13}\text{CO}_2$  molecule. Here, the  $^{12}\text{CO}_2$  are plotted at the left and the  $^{13}\text{CO}_2$  molecules are plotted on the right hand side of the vertical dashed white line. Fig. 2d shows that there is now a competition between exciting  $^{12}\text{CO}_2$  and  $^{13}\text{CO}_2$  molecules, as molecules of both isotopes exhibit intense, red-shifted peaks.

This conclusion is illustrated quantitatively in Fig. 3a, where we plot the dynamics of the average C=O bond potential energy (minus the thermal energy  $k_B T$ ) per  $^{12}\text{CO}_2$  (gray line) or  $^{13}\text{CO}_2$  (red line) molecule after the strong LP excitation. Due to the LP excitation [where the time window of the pulse ( $0.1 < t < 0.6 \text{ ps}$ ) is represented with a yellow region], the vibrational energy of the  $^{13}\text{CO}_2$  solute molecules can reach roughly four times that of the  $^{12}\text{CO}_2$  solvent molecules and each solute molecule can absorb roughly a vibrational quantum ( $\sim 2 \times 10^3 \text{ cm}^{-1}$ ) of the input energy. Note that Fig. 3a is drawn with a logarithmic scale; see the black arrow which denotes the energy difference. By contrast, outside the cavity, when the  $^{13}\text{C}=\text{O}$  asymmetric stretch of the liquid mixture is resonantly excited by the same pulse (Fig. 3c),

the  $^{13}\text{CO}_2$  vibrational energy reaches roughly twice the energy of the  $^{12}\text{CO}_2$  solvent molecules, and the energy absorption of each solute molecule is roughly half a vibrational quantum ( $\sim 10^3 \text{ cm}^{-1}$ ). Our finding indicates that the cavity environment can meaningfully improve the selectivity and also the absolute value of solute excitation by a factor of two (though perhaps not a huge effect).

## C. Improving the selectivity of energy transfer to solute molecules by tuning the Rabi splitting

In order to improve the selectivity of energy transfer from the LP, we need to both (i) suppress the energy transfer to the  $^{12}\text{CO}_2$  solvent molecules and also (ii) enhance the energy transfer to the  $^{13}\text{CO}_2$  solute molecules. As mentioned above, the nonuniform polaritonic energy transfer stems from polariton-enhanced molecular nonlinear absorption, a mechanism which requires twice the LP frequency to roughly match the  $0 \rightarrow 2$  vibrational transition. In other words, by changing the LP frequency relative to the vibration of one molecular species, we can enhance or suppress polaritonic energy transfer to that molecular species according to a frequency match or mismatch.

Let us first focus on the side of  $^{12}\text{CO}_2$  molecules and investigate how to suppress the energy transfer to the  $^{12}\text{CO}_2$  molecules with an increased Rabi splitting. For a pure liquid  $^{12}\text{CO}_2$  system, when the effective light-matter coupling strength is increased from  $\tilde{\epsilon} = 2 \times 10^{-4}$  a.u. to  $\tilde{\epsilon} = 4 \times 10^{-4}$  a.u., the red line in Fig. 2e plots the equilibrium IR spectrum inside the cavity with  $\omega_c = 2320 \text{ cm}^{-1}$ . For the larger light-matter coupling ( $\tilde{\epsilon} = 4 \times 10^{-4}$  a.u.), the Rabi splitting increases by a factor of two and the LP frequency red-shifts from  $2241 \text{ cm}^{-1}$  (in Figs. 2a-d) to  $2177 \text{ cm}^{-1}$ . Now, as shown in Fig. 2f, after a resonant excitation of the LP with a strong laser pulse, polaritonic energy transfer to  $^{12}\text{CO}_2$  molecules is largely suppressed compared with Fig. 2b. The suppression of polaritonic energy transfer is consistent with a longer LP lifetime (2.9 ps) relative to that in Fig. 2b (0.2 ps); this longer LP lifetime can be observed in Fig. 2f by visualizing the near uniform intensity among all molecules at the LP frequency (positioned by the red arrow) over the time scale 1-6 ps, which corresponds to a long lived molecular bright state.

Second, consider the case where the liquid mixture of 4.63 %  $^{13}\text{CO}_2$  in a  $^{12}\text{CO}_2$  solution experiences a larger light-matter coupling (with  $\tilde{\epsilon} = 4 \times 10^{-4}$  a.u.). Because the concentration of the  $^{13}\text{CO}_2$  solute molecules is small, the equilibrium IR spectrum inside the cavity (Fig. 2g) remains unchanged compared with the case of pure liquid  $^{12}\text{CO}_2$  (Fig. 2e). After resonantly exciting the LP with a strong laser pulse, as shown in Fig. 2h, we find that the polaritonic energy mostly transfers to the  $^{13}\text{CO}_2$  molecules (on the right hand side of the vertical dashed white line). Quantitatively speaking, Fig. 3b plots the corresponding dynamics of the average C=O bond po-

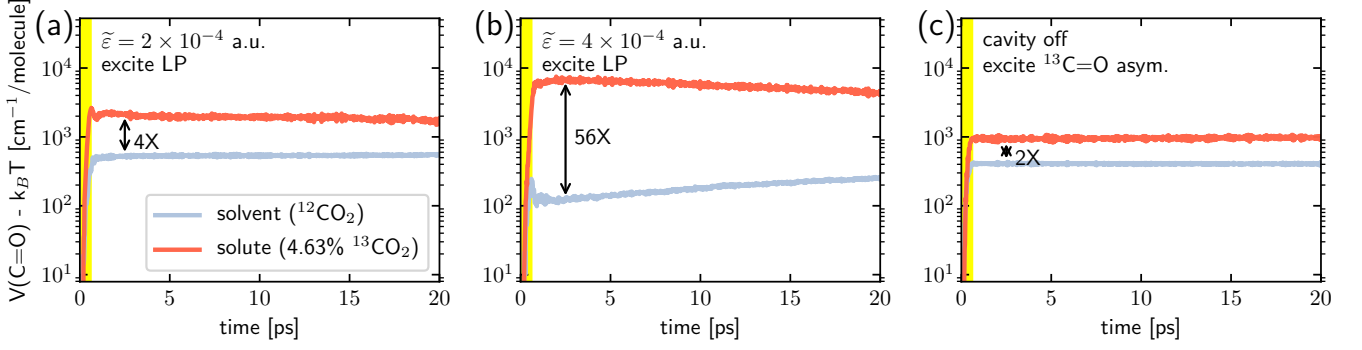


FIG. 3. Time-resolved dynamics for the average C=O bond potential energy per solvent ( $^{12}\text{CO}_2$ , gray line) or solute molecule (4.63%  $^{13}\text{CO}_2$ , red line). Three conditions are compared: (a)  $\tilde{\epsilon} = 2 \times 10^{-4}$  a.u. after exciting the LP at  $2241 \text{ cm}^{-1}$  (the same as Fig. 2d); (b)  $\tilde{\epsilon} = 4 \times 10^{-4}$  a.u. after exciting the LP at  $2177 \text{ cm}^{-1}$  (the same as Fig. 2h); and (c) outside the cavity after exciting the  $^{13}\text{C}=\text{O}$  asymmetric stretch at  $2262 \text{ cm}^{-1}$ . In each subplot, the  $y$ -axis is plotted in a logarithmic scale, and the yellow region denotes the time window ( $0.1 < t < 0.6$  ps) during which the external pulse is applied.

tential energy for the solute and solvent molecules. Here, within the time window of the laser pulse ( $t < 1$  ps), the solute molecules can be excited to a state of roughly three vibrational quanta (recall that the frequency of the C=O asymmetric stretch is roughly  $\sim 2 \times 10^3 \text{ cm}^{-1}$ ), which is six times of the outside-cavity solute energy absorption (Fig. 3c). As far as selectivity is considered, within  $t < 5$  ps, the solute molecules can absorb an energy 56 times larger than the solvent molecules (see the black arrow), a difference which is one-order-of-magnitude larger than the case of outside the cavity (Fig. 3c). In short, although we found above that, when  $\tilde{\epsilon} = 2 \times 10^{-4}$  a.u., there is a competition between the polaritonic energy transfer to  $^{12}\text{CO}_2$  and  $^{13}\text{CO}_2$  molecules, we now find that when  $\tilde{\epsilon} = 4 \times 10^{-4}$  a.u.,  $^{13}\text{CO}_2$  clearly wins.

The high selectivity of this polaritonic energy transfer to the solute molecules can be explained as follows. First, since the LP frequency is unchanged compared with the pure liquid  $^{12}\text{CO}_2$  system in Fig. 2e, polariton-enhanced molecular nonlinear absorption for the  $^{12}\text{CO}_2$  solvent molecules remains greatly suppressed, which is analogous to Fig. 2f. Second, for the larger Rabi splitting, the vibrational frequency difference between the LP and  $^{13}\text{C}=\text{O}$  asymmetric stretch (see red and gray lines in Fig. 2g) is suitable to allow for polariton-enhanced molecular nonlinear absorption of the solute molecules. This statement is consistent with the shortened LP lifetime in Fig. 2h (0.6 ps) as compared with  $\tau_{\text{LP}} = 2.9$  ps in Fig. 2f. All together, these two facts lead to a high selectivity in energy transfer.

#### D. Dependence on system size and solute concentration

One important issue we must address is the dependence of polaritonic energy transfer on molecular system size. This study is necessary because usual VSC setups in experiments (e.g., Fabry-Pérot microcavities) usually contain a macroscopic number of molecules, while

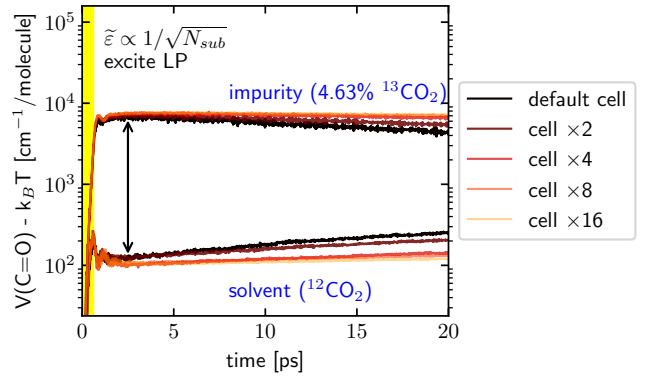


FIG. 4. Effects of the molecular system size on the dynamics of C=O bond potential energy for a fixed Rabi splitting, molecular density, and solute concentration. Black lines correspond to the data in Fig. 3b ( $N_{\text{sub}} = 216$ ), and the lines from dark red to orange represent increasing molecular systems where  $N_{\text{sub}}$  is increased by a factor of  $N$  ( $N = 2, 4, 8, 16$ ). Note that the selective polaritonic energy transfer to the  $^{13}\text{CO}_2$  solute molecules is fairly robust against molecular system size, indicating that the current finding may hold for collective VSC with large cavity volumes but under the same Rabi splitting, i.e., smaller  $\tilde{\epsilon}$ ; see text below for an explanation of the system size dependence.

we have only simulated a molecular system of  $N_{\text{sub}} = 216$  coupled to the cavity. Therefore, we must check how our conclusions vis a vis VSC effects depend on molecular system size.

Following the approach from Refs. [18], in Fig. 3b, we enlarge the molecular system by simultaneously increasing both the number of  $^{13}\text{CO}_2$  and  $^{12}\text{CO}_2$  molecules (maintaining a constant proportion) and we decrease the light-matter coupling strength ( $\tilde{\epsilon}$ ); these two effects are chosen in a balanced manner so as to keep the molecular density and Rabi splitting the same as in Figs. 2g,h. For systems with different sizes, after the same strong excitation of the LP, Fig. 4 plots the dynamics of the average



C=O bond potential energy for the  $^{13}\text{CO}_2$  and  $^{12}\text{CO}_2$  molecules. Here, the top and bottom lines denote the dynamics of  $^{13}\text{CO}_2$  and  $^{12}\text{CO}_2$  molecules, respectively. Lines with different colors (from black to orange) denote molecular systems of different sizes (from  $N_{\text{sub}} = 216$  to  $N_{\text{sub}} = 216 \times 16$ ). Note that after the pulse, the  $^{13}\text{CO}_2$  molecules are hot and start to cool down, while the weakly excited  $^{12}\text{CO}_2$  molecules start to heat up. Fig. 4 also clearly shows that, although the later-time vibrational relaxation and energy transfer dynamics ( $t > 5$  ps) can depend on the size of the molecular system [26], we do observe a consistent selective polaritonic energy transfer behavior at early times ( $t < 5$  ps) for all molecular system sizes. Therefore, we tentatively conclude that our numerical findings here should be observable in cavities with different volumes, including Fabry-Pérot microcavities (that are usually used to study collective VSC) and plasmonic cavities, an emerging platform for studying VSC [27, 28].

Note that the robustness of the early-time polaritonic decay dynamics against the system size can be rationalized by, e.g., Fermi's golden rule calculations. Although the interaction between the polariton and each dark mode scales with  $1/N$  (where  $N$  denotes the total molecular number) via intermolecular interactions, since there are  $N - 1$  dark modes which allow polaritonic energy transfer (or dephasing), when Fermi's golden rule is used to describe the polaritonic relaxation dynamics, the  $1/N$  and  $N - 1$  factors cancel with each other, leading to consistent early-time dynamics during polaritonic relaxation versus the system size. With the same argument, for the later-time vibrational relaxation and energy transfer dynamics (when the polariton is completely decayed), the cavity plays a role by allowing the following energy transfer channel:  $^{13}\text{CO}_2 \rightarrow \text{polaritons} \rightarrow ^{12}\text{CO}_2$ . For the first step ( $^{13}\text{CO}_2 \rightarrow \text{polaritons}$ ), since there are not  $N$  final states (i.e. with only *two* polaritons), polaritons no longer play an important role once the system size is very large, leading to slower vibrational relaxation and energy transfer dynamics in later times; see Ref. [26] for a detailed study.

Finally, in Fig. 5, we plot the dynamics of averaged C=O bond potential energy per  $^{13}\text{CO}_2$  solute or  $^{12}\text{CO}_2$  solvent molecule as a function of time for different system sizes — but now with a fixed number (10) of solute molecules. In other words, we increase only the number of  $^{12}\text{CO}_2$  solvent molecules (so that the solute concentration is decreased). For all curves, as above, the total Rabi splitting is kept constant by decreasing the effective coupling strength  $\tilde{\epsilon}$ , which corresponds physically to placing the system in a larger volume cavity.

Perhaps counter-intuitively, Fig. 5 shows that the C=O bond energy of both the solvent and solute molecules increases as the number of solvent molecules increases. These findings can be explained as follows. On the one hand, as for the solute molecules, when the number of solvent molecules increases, the total transition dipole of the solvent bright mode also increases, such that the total amount of energy absorbed through the po-

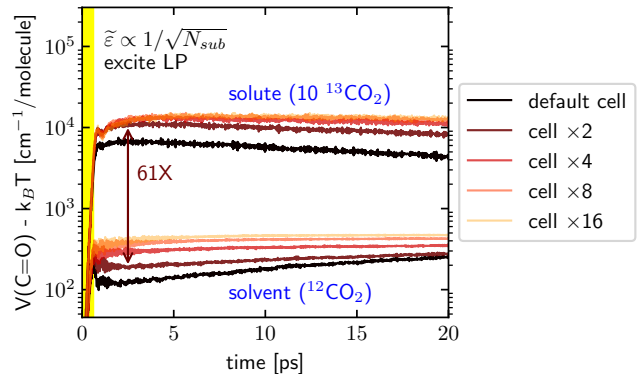


FIG. 5. The same plot as Fig. 4 except for that the  $^{13}\text{CO}_2$  solute molecular number is fixed as 10 when the system size enlarges. Note that, when the system size is increased (or when the solute concentration is decreased), both the solvent and solute molecules are more heavily pumped under the same IR excitation of the LP. See text for details of this counter-intuitive feature.

lariton grows when the same incident pulse is applied — and each solute molecule will recover more energy from the polariton through the nonlinear channel (since the energy absorbed by the polariton divided by the solute number grows). On the other hand, when the concentration of the solute decreases (under larger system sizes), the pumped solvent polariton cannot efficiently transfer energy to its favorite acceptor (the solute), such that the polariton transfers more energy to the solvent molecules. Finally, with regards to selectivity (i.e., energy of solute divided by energy of solvent), these two effects clearly work against each other. Empirically, we find that the selectivity reaches a maximum value of 61 times (see the vertical brown arrow) and the solute excitation can exceed  $10^4 \text{ cm}^{-1}$  ( $4 \sim 5$  quanta) when we double the system size (i.e. we add slightly more than two times the number of solvent molecules, so that the solute concentration becomes 2.32%, the brown lines).

The findings above cannot be achieved outside a cavity. For example, on the one hand, when the solvent bright mode is pumped outside a cavity, since the excited bright mode dephases on a much faster timescale than the polaritons, and because there is no resonance conditions between the solvent bright mode and the solute, energy transfer from the solvent to solute is not efficient and occurs on a much longer timescale than 1 ps. On the other hand, when the solute vibration is directly excited outside the cavity (see Fig. 3c), the energy absorbed by the system is much smaller than the inside-cavity case (where energy absorption is dominated by the solvent polariton).

#### IV. CONCLUSION

To summarize, we have numerically demonstrated that energy from a strong IR laser pulse can be selectively transferred to solute molecules by pumping the LP of

the solvent molecules. This selective energy transfer behavior requires the LP to have an appropriate frequency to selectively enhance molecular nonlinear absorption for the solute (but not solvent) molecules and can be optimized by changing the solute concentration. Consequently, the transient vibrational energy difference between the solute and the solvent molecules can exceed the free-space case by more than one order of magnitude. Since our CavMD simulations have shown some key agreements with VSC experiments (including the signature of polariton-enhanced molecular nonlinear absorption), and because the current finding of selective energy transfer to the solute molecules is robust against the cav-

ity volume, we believe that this finding is also amenable to experimental verification. In principle, our finding might be one route to IR laser-controlled chemistry on an electronic ground-state surface, which remains difficult to achieve in liquid phase. Lastly, we emphasize that the energy transfer from the polariton (which is predominately composed of the solvent bright mode and the cavity mode) to the solute molecules is extremely fast in our simulations above (within 1 ps); this ultrashort timescale highlights how VSC in a cavity can greatly accelerate rates of intermolecular vibrational energy transfer and underscores the future possibility of using collective VSC to modify molecular properties.

- 
- [1] D. Maas, D. Duncan, R. Vrijen, W. van der Zande, and L. Noordam, Vibrational ladder climbing in NO by (sub)picosecond frequency-chirped infrared laser pulses, *Chem. Phys. Lett.* **290**, 75 (1998).
  - [2] J. C. Owrutsky, D. Raftery, and R. M. Hochstrasser, Vibrational Relaxation Dynamics in Solutions, *Annu. Rev. Phys. Chem.* **45**, 519 (1994).
  - [3] T. Stensitzki, Y. Yang, V. Kozich, A. A. Ahmed, F. Kössl, O. Kühn, and K. Heyne, Acceleration of a ground-state reaction by selective femtosecond-infrared-laser-pulse excitation, *Nat. Chem.* **10**, 126 (2018).
  - [4] K. Heyne and O. Kühn, Infrared Laser Excitation Controlled Reaction Acceleration in the Electronic Ground State, *J. Am. Chem. Soc.* **141**, 11730 (2019).
  - [5] M. Delor, P. A. Scattergood, I. V. Sazanovich, A. W. Parker, G. M. Greetham, A. J. H. M. Meijer, M. Towrie, and J. A. Weinstein, Toward control of electron transfer in donor-acceptor molecules by bond-specific infrared excitation, *Science* **346**, 1492 (2014).
  - [6] A. Shalabney, J. George, J. Hutchison, G. Pupillo, C. Genet, and T. W. Ebbesen, Coherent coupling of molecular resonators with a microcavity mode, *Nat. Commun.* **6**, 5981 (2015).
  - [7] J. George, A. Shalabney, J. A. Hutchison, C. Genet, and T. W. Ebbesen, Liquid-Phase Vibrational Strong Coupling, *J. Phys. Chem. Lett.* **6**, 1027 (2015).
  - [8] A. Thomas, J. George, A. Shalabney, M. Dryzhakov, S. J. Varma, J. Moran, T. Chervy, X. Zhong, E. Devaux, C. Genet, J. A. Hutchison, and T. W. Ebbesen, Ground-State Chemical Reactivity under Vibrational Coupling to the Vacuum Electromagnetic Field, *Angew. Chemie Int. Ed.* **55**, 11462 (2016).
  - [9] R. M. A. Vergauwe, A. Thomas, K. Nagarajan, A. Shalabney, J. George, T. Chervy, M. Seidel, E. Devaux, V. Torbeev, and T. W. Ebbesen, Modification of Enzyme Activity by Vibrational Strong Coupling of Water, *Angew. Chemie Int. Ed.* **58**, 15324 (2019).
  - [10] J. Lather, P. Bhatt, A. Thomas, T. W. Ebbesen, and J. George, Cavity Catalysis by Cooperative Vibrational Strong Coupling of Reactant and Solvent Molecules, *Angew. Chemie Int. Ed.* **58**, 10635 (2019).
  - [11] A. Thomas, L. Lethuillier-Karl, K. Nagarajan, R. M. A. Vergauwe, J. George, T. Chervy, A. Shalabney, E. Devaux, C. Genet, J. Moran, and T. W. Ebbesen, Tilting a ground-state reactivity landscape by vibrational strong coupling, *Science* **363**, 615 (2019).
  - [12] J. Galego, C. Climent, F. J. Garcia-Vidal, and J. Feist, Cavity Casimir-Polder Forces and Their Effects in Ground-State Chemical Reactivity, *Phys. Rev. X* **9**, 021057 (2019).
  - [13] T. E. Li, A. Nitzan, and J. E. Subotnik, On the origin of ground-state vacuum-field catalysis: Equilibrium consideration, *J. Chem. Phys.* **152**, 234107 (2020).
  - [14] J. A. Campos-Gonzalez-Angulo and J. Yuen-Zhou, Polaritonic normal modes in transition state theory, *J. Chem. Phys.* **152**, 161101 (2020).
  - [15] X. Li, A. Mandal, and P. Huo, Cavity frequency-dependent theory for vibrational polariton chemistry, *Nat. Commun.* **12**, 1315 (2021).
  - [16] T. E. Li, J. E. Subotnik, and A. Nitzan, Cavity molecular dynamics simulations of liquid water under vibrational ultrastrong coupling, *Proc. Natl. Acad. Sci.* **117**, 18324 (2020).
  - [17] B. Xiang, R. F. Ribeiro, M. Du, L. Chen, Z. Yang, J. Wang, J. Yuen-Zhou, and W. Xiong, Intermolecular vibrational energy transfer enabled by microcavity strong light-matter coupling, *Science* **368**, 665 (2020).
  - [18] T. E. Li, A. Nitzan, and J. E. Subotnik, Cavity molecular dynamics simulations of vibrational polariton-enhanced molecular nonlinear absorption, *J. Chem. Phys.* **154**, 094124 (2021).
  - [19] B. Xiang, R. F. Ribeiro, A. D. Dunkelberger, J. Wang, Y. Li, B. S. Simpkins, J. C. Owrutsky, J. Yuen-Zhou, and W. Xiong, Two-dimensional infrared spectroscopy of vibrational polaritons, *Proc. Natl. Acad. Sci.* **115**, 4845 (2018).
  - [20] B. Xiang, R. F. Ribeiro, L. Chen, J. Wang, M. Du, J. Yuen-Zhou, and W. Xiong, State-Selective Polariton to Dark State Relaxation Dynamics, *J. Phys. Chem. A* **123**, 5918 (2019).
  - [21] V. Kapil, M. Rossi, O. Marsalek, R. Petraglia, Y. Litman, T. Spura, B. Cheng, A. Cuzzocrea, R. H. Meißner, D. M. Wilkins, B. A. Helfrecht, P. Juda, S. P. Bienvenue, W. Fang, J. Kessler, I. Poltavsky, S. Vandenbrande, J. Wieme, C. Corminboeuf, T. D. Kühne, D. E. Manolopoulos, T. E. Markland, J. O. Richardson, A. Tkatchenko, G. A. Tribello, V. Van Speybroeck, and M. Ceriotti, i-PI 2.0: A universal force engine for advanced molecular simulations, *Comput. Phys. Commun.* **236**, 214 (2019).
  - [22] S. Plimpton, Fast Parallel Algorithms for Short-Range Molecular Dynamics, *J. Comput. Phys.* **117**, 1 (1995).

- [23] T. E. Li, Cavity Molecular Dynamics Simulations Tool Sets, <https://github.com/TaoELi/cavity-md-ipi> (2020).
- [24] M.-P. Gaigeot and M. Sprik, Ab Initio Molecular Dynamics Computation of the Infrared Spectrum of Aqueous Uracil, *J. Phys. Chem. B* **107**, 10344 (2003).
- [25] R. F. Ribeiro, J. A. Campos-Gonzalez-Angulo, N. C. Giebink, W. Xiong, and J. Yuen-Zhou, Enhanced optical nonlinearities under strong light-matter coupling, (2020), arXiv:2006.08519.
- [26] T. E. Li, A. Nitzan, and J. E. Subotnik, Collective vibrational strong coupling effects on molecular vibrational relaxation and energy transfer: Numerical insights via cavity molecular dynamics simulations, (2021), arXiv:2103.06749.
- [27] Z. T. Brawley, S. D. Storm, D. A. Contreras Mora, M. Pelton, and M. Sheldon, Angle-independent plasmonic substrates for multi-mode vibrational strong coupling with molecular thin films, *J. Chem. Phys.* **154**, 104305 (2021).
- [28] D. Yoo, F. de León-Pérez, M. Pelton, I.-H. Lee, D. A. Mohr, M. B. Raschke, J. D. Caldwell, L. Martín-Moreno, and S.-H. Oh, Ultrastrong plasmon-phonon coupling via epsilon-near-zero nanocavities, *Nat. Photonics* **15**, 125 (2021).